# Competitive Adsorption of Cu, Ni, Pb, and Cd
# from Aqueous Solution Onto Fly Ash-Based Linde F(K) Zeolite

***Cheng, Ting***

*Department of City Science, Jiangsu City Vocational College, Nanjing 210036, CHINA*

***Chen, Chen*\*+**

*School of Environmental and Chemical Engineering, Jiangsu University of Science and Technology, Zhenjiang 212003, CHINA*

***Tang, Rong; Han, Cheng-Hui***

*Department of City Science, Jiangsu City Vocational College, Nanjing 210036, CHINA*

***Tian, Yuan***

*School of Environmental and Chemical Engineering, Jiangsu University of Science and Technology, Zhenjiang 212003, CHINA*

**ABSTRACT:** *The reaction of fly ash with a KOH solution was used to synthesize Linde F(K) zeolite, following which Fourier transform infrared spectroscopy were used to characterize the crystalline material. The competitive adsorption of Cu, Ni, Pb, and Cd onto this zeolite was subsequently studied in quaternary solution systems. The results show that the metal removal rates gradually increase with increases in the pH of the adsorption solution until reaching an asymptotic value. During the early stages of adsorption, the metal removal rate is very rapid, after which it gradually decreases. The overall adsorption efficiency order is Pb > Cd > Cu > Ni. The adsorption process is best represented by pseudo-second-order kinetics and an internal surface diffusion model. The primary adsorption process, which takes place between approximately 1 to 2 min and 40 min, appears to be controlled by internal surface diffusion.*

**KEYWORDS:** *Heavy metal; Competitive adsorption; Zeolite; Fly ash.*

## INTRODUCTION

As a consequence of rapid economic development, environmental pollution has become a major problem in many developing countries, including China. Special attention has been accorded to water pollution because of the potential impact on human health [1]. Compared with other organic and inorganic pollutants, the heavy metal

61

wastewater produced by metal plating facilities, as well as during the production of paints, pigments, ammunition, ceramics, and glass, is of importance because of the potential for cumulative environmental effects [2-4]. According to the list of priority pollutants published by the US Environmental Protection Agency, various heavy metals, including Cu, Pb, Cd, and Ni, represent serious toxicity hazards. These heavy metals resist biodegradation and tend to accumulate in living organisms, leading to several diseases that affect the kidney, nervous, hematopoietic, and gastrointestinal systems [5-7]. Based on this health hazard, the Chinese government has stipulated that the concentrations of Cu, Pb, Cd, and Ni in discharged wastewater must be below 0.5, 1.0, 0.1, and 1.0 mg/L, respectively. Therefore, it is necessary to develop more efficient methods to remove these heavy metals from aquatic environments.

Currently, much effort is being devoted to the removal of heavy metals from aqueous solutions. Conventional water treatment technologies for heavy metals include adsorption, chemical precipitation and ion exchange, coagulation, electrochemistry, and membrane separation [8-10]. Among these commonly used methods, adsorption is believed to be perhaps the most highly efficient, cost-effective, versatile and facile [11], and is widely used for the removal of heavy metals from wastewater [12-16]. For this reason, extensive research has been applied to the search for a suitable and relatively cheap adsorbent and there is an increasing focus on adsorbents synthesized from low-cost materials such as industrial byproducts or waste streams [17-21].

Fly ash is a solid waste generated by coal-fired power plants. In 2015, such plants in China alone will produce about 58 million tons of fly ash, only approximately 60% of which will be reused in various applications. The majority of the remaining material will be disposed of in landfills that occupy otherwise cultivatable land and that can generate both air and groundwater pollution. Using fly ash as a raw material to synthesis adsorbents for heavy metals would not only decrease the cost of adsorption technology but would also solve the environmental problems associated with waste fly ash disposal. Over the past several years, fly ash-based zeolites have been shown to function as effective adsorbents for the removal of heavy metals. The synthetic zeolites 4A and Na–P1 produced from fly ash were applied

to the treatment of swine wastewater by Cardoso [17], while Grela used coal-fired boiler fly ash to synthesize zeolites and reported the thermal behavior and physical characteristics of these materials [22]. Cardoso suggested that the zeolite Na-P1, synthesized from fly ash under mild conditions, could be applied for wastewater treatment[23]. Belviso used fly ash as a raw material to synthesize hydrothermal synthetic zeolites that showed a remarkable affinity for the removal of Mn from aqueous solutions[24].

Linde F(K) zeolite (hereafter referred as the "zeolite") is a product obtained from the hydrothermal reaction between fly ash and a highly concentrated KOH solution. In our previous work, we determined that this zeolite is a promising adsorbent for heavy metals removal. Adsorption kinetics and isotherm studies were carried out for the adsorptions of Pb, Cd, Zn, and Ni from aqueous solutions on this material, and these studies confirmed high adsorption rates and determined the Langmuir adsorption amounts for these heavy metal ions [25, 26]. However, industrial wastewater normally contains more than one heavy metal, and the coexistence of many heavy metals in solution could affect the adsorption capacity of the individual metals. Therefore, the adsorption results from single-component systems cannot necessarily be applied to multi-component systems, and the competitive adsorption behavior of heavy metals must be studied. The selectivity and affinity of heavy metals on a zeolite and the competition between the metal ions for adsorption sites both have to be determined.

The main objective of the present work was to evaluate the feasibility of removing Cu, Pb, Cd, and Ni from aqueous solutions using Linde F(K) zeolite prepared from fly ash in a multi-component system, and to establish an applicable adsorption kinetics model. Different parameters influencing the adsorption behavior in this four-component system were examined, including contact time, pH, zeolite concentration, and temperature. Lagergren pseudo-first-order, pseudo-second-order, internal surface diffusion, and external surface diffusion models were all used to assess the adsorption kinetics.

## EXPERIMENTAL SECTION
### Materials
An aqueous solution of Cu, Pb, Cd, and Ni was prepared by dissolving $Cu(NO_3)_2$, $Pb(NO_3)_2$, $Cd(NO_3)_2$,

and $Ni(NO_3)_2$ in deionized (DI) water in sufficient quantities, so as to obtain concentrations of 100 mg/L of each metal ion. The alkaline solution used for zeolite synthesis was prepared by dissolving KOH in DI water. The solutions employed to adjust the adsorption solution pH were obtained by dissolving either NaOH or $HNO_3$ (0.01 mol/L) in DI water. All chemicals used in our experiments were analytical reagent grade and were purchased from the China National Pharmaceutical Group Corporation. The Linde F(K) zeolite was synthesized by reacting fly ash with a KOH solution, as reported in our previous publications [25,26].

### Adsorption of heavy metals

The adsorption experiments were conducted as typical batch trials. In each trial, a quantity of the zeolite was dispersed in 10 mL of the metal ions solution in a 20 mL Teflon bottle. The bottles were subsequently immersed in a water bath and agitated at 200 rpm. Following adsorption, each dispersion was filtered through a 0.45-μm membrane and the Cu, Pb, Cd, and Ni concentrations in the filtered solution were determined by atomic absorption spectrophotometry using an AA240FS instrument. The initial concentrations of all metal ions are 100mg/L. The metal uptake ($q_e$) was calculated using the following mass balance equation:

$$q_e = \frac{(C_0 - C_{eq})V}{m} \qquad (1)$$

where $q_e$ (mg/g) is the mass of metal ions adsorbed per unit mass of the sorbent, $V$ (L) is the sample volume, $C_0$ (mg/L) and $C_e$ (mg/L) are the initial and equilibrium concentrations, respectively, and $m$ (g) is the mass of the sorbent.

The effects of solution pH on adsorption were assessed over the pH range of 2–8. The pH of each solution was adjusted by the addition of 0.01 mol/L NaOH and/or 0.01 mol/L $HNO_3$ solutions and measured using a Q/GHSC 1544-2009 pH meter. During these trials, the contact time was 8 h, the zeolite concentration was 2 g/L, and the solution temperature was 25 °C. The surface zeta potential of zeolite is determined by JS94H microiontophoresis apparatus (POWEREACH). The effects of zeolite concentration on adsorption were determined over the range of 0.25–9 g/L zeolite at a pH of 6 and an adsorption contact time of 8 h, applying
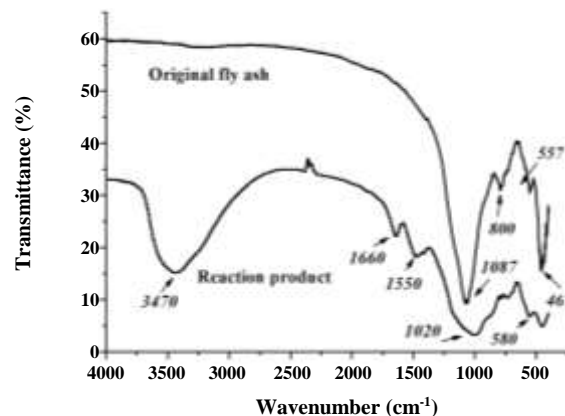


**Fig. 1: FT-IR spectra of the original fly ash and the reaction product.**

temperatures of 25–45 °C. The effects of contact time and temperature on adsorption were examined using times of 0.5–6 h at pH 6 and a zeolite concentration of 2 g/L with temperatures ranging from 25 to 45 °C.

## RESULTS AND DISCUSSIONS
### FT-IR

Fig. 1 presents the FT-IR spectra of the original fly ash and the reaction product. Intense peaks are seen at 1087, 800, 557, and 467 cm⁻¹ and are attributed to T–O bond (where T is Si or Al) stretching, quartz double, mullite, and $SiO_4$ tetrahedron (O–Si–O) deformation bands, respectively [27]. The intense but broad bands at approximately 3470, 1660, and 1550 cm⁻¹ could result from the stretching and bending vibrations of O–H in the reaction products [28], and so are believed to result from the hydrothermal reaction between the fly ash and the alkaline solution. Several new bands appear in the product, at 1020 and 580 cm⁻¹, owing to the Si(Al)–O–Si(Al) stretching vibration and the O–Si(Al)–O bending mode [29], indicating the formation of Si(Al)–O tetrahedra in the Linde F(K) zeolite.

### Effect of initial solution pH

The initial pH of the adsorption solution affects both the protonation of the adsorbent surface groups and the degree of ionization of the metals, and thus can significantly affect the adsorption process. It is therefore beneficial to determine the optimal pH that generates the maximum adsorption efficiency. Fig. 2 summarizes the effects of pH on Cu, Ni, Cd, and Pb adsorption
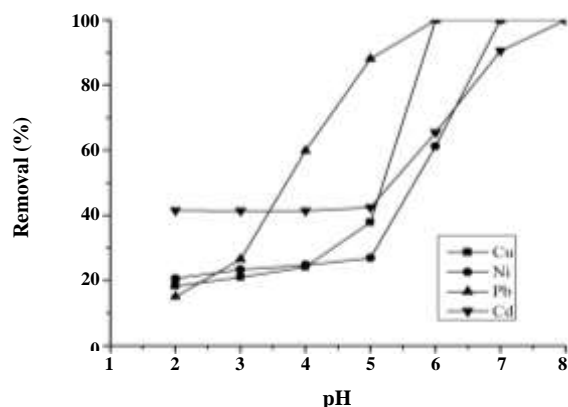
63

*Fig. 2: Effects of pH on the adsorption of Cu, Ni, Pb, and Cd on the zeolite.*



*Fig. 3: Surface zeta potential of zeolite under different pH solution.*

on the Linde F(K) zeolite. To avoid precipitation of metal hydroxides at high pH (typically above 8), the experiments were conducted at pH values ranging from 2 to 8.

It can be seen that the adsorption efficiency was lowest in strongly acidic solutions and increased with increases in the initial solution pH until reaching an asymptotic value. All the metal ions exhibited maximum adsorption capacity at a pH in the range of 6–7. The competitive relationship between the metal ions is also evident from these data. At the same initial solution pH, the adsorption efficiency order is Pb > Cd/ Cu > Ni. This result implies that the degree of ionization of the metals could impact the adsorption rate and that Pb ions have the highest affinity for the zeolite surface.

These results can be explained by considering the surface zeta potential of zeolite (Fig. 3). At an initial solution pH below about 5, the surface of the zeolite is positively charged, and so the adsorption capacity of the zeolite for positive metal ions is severely restricted. In addition, the H$^+$ ions in solution will also effectively compete with metal ions for zeolite adsorption sites and so less acidic solutions should exhibit greater adsorption. On the contrary, at an initial solution pH above the about 5, the negatively charged zeolite surface will have a stronger coordinative affinity towards metal cations (Fig. 4). In such cases, the electrostatic forces of attraction allow carboxylate ions on the zeolite to capture the M$^{2+}$ ions through surface complexation, forming chelate complexes.

### Effect of contact time and adsorption temperature

The effects of contact time and adsorption temperature on the removal of metal ions are presented in Fig. 5.
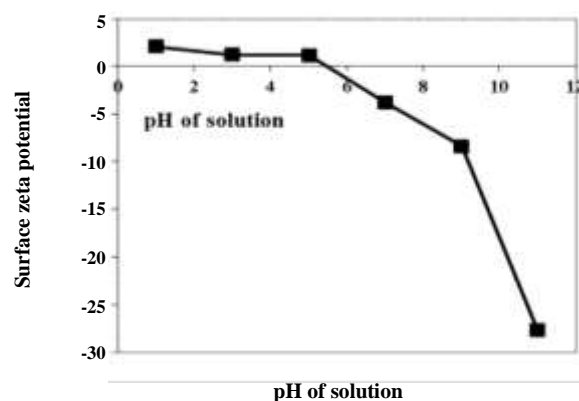
These results show that the initial metal removal rate was very rapid and then gradually decreased until equilibrium was attained. As an example, at 35 °C, 88.4% Pb (89.6% of the maximum adsorption), 41.5% Cd (95.9%), 32.1% Cu (81.7%), and 15.9% Ni (85.9%) were removed from the solution within a contact time of only 10 min. The uptake of metal ions on the zeolite was thus very fast and the Pb ions again exhibit the highest affinity. It is noteworthy that the adsorption efficiency order is Pb > Cd/Cu > Ni at each temperature and that the removal rate of each of the metal ions increased sharply as the adsorption temperature was raised. At 25 °C, the proportional uptakes were 89.2% (Pb), 41.9% (Cd), 34.2% (Cu), and 15.9% (Ni) after 1 h, while values of 97.6% (Pb), 42.6% (Cd), 41.1% (Cu), and 23.5% (Ni) were obtained after 1 h at 45 °C.

### Adsorption kinetics

During adsorption kinetics analyses, both pseudo-first-order and pseudo-second-order kinetic models were applied to the experimental data. These two models were employed to assist in evaluating the adsorption mechanism and to identify the potential rate-controlling steps.

The Lagergren pseudo-first-order model can be summarized as [30] :

$$\ln(q_e - q_t) = \ln q_{cal} - k_1 t \qquad (2)$$

Where $q_e$ is the equilibrium adsorption amount of M (heavy metal) on the zeolite (mg/g), $q_t$ is the adsorption amount of M on the zeolite at time $t$ (mg/g), $k_1$ (1/min) is the rate constant of the first-order model, and $t$ is contact time.
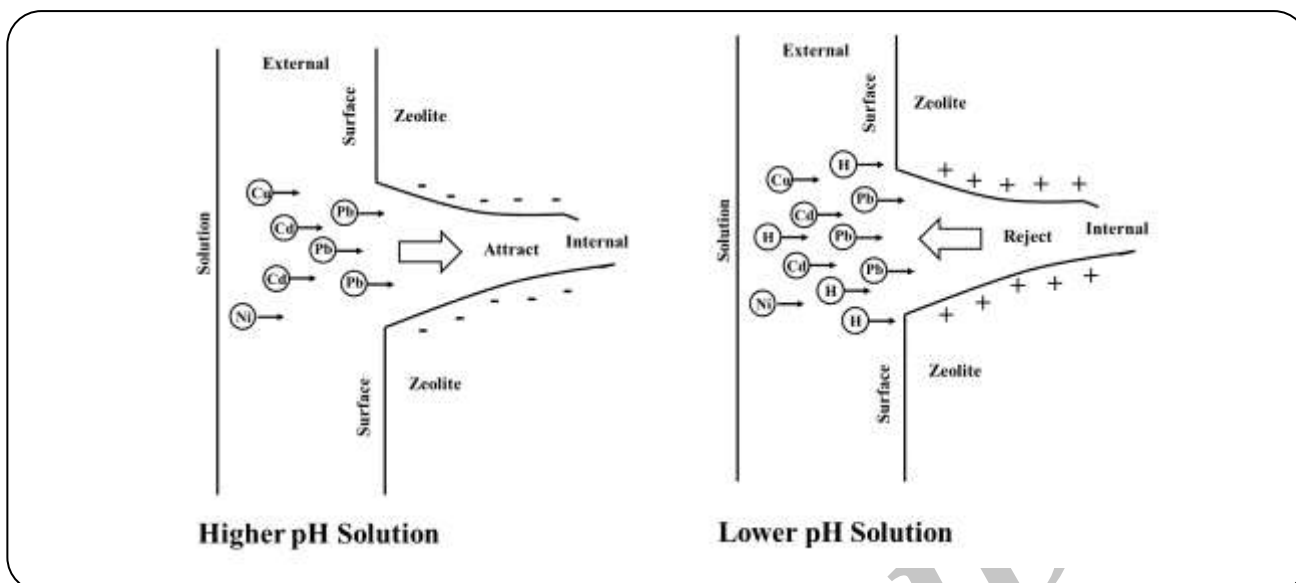
64

*Fig. 4: Adsorption model of metals on the zeolite under different pH solution.*

The Ho & McKay pseudo-second-order model is summarized by [31, 32]:

$$\frac{t}{q} = \frac{1}{k_2 q_{cal}^2} + \frac{t}{q_{cal}} \tag{3}$$

Where $k_2$ (g/mg·min) is the rate constant of the second-order model.

Figure 6 and Table 1 display the kinetics fitting graphs and results. Based on the calculated $R^2$ (correlation coefficient) values, the adsorption of metal ions on the zeolite appears to more closely match the pseudo-second-order kinetic model than the pseudo-first-order model. The optimal model can be chosen based on the Root Mean Square Error (RMSE), defined as follows [33]:

$$RMSE = \sqrt{\frac{\sum_{1}^{N}(q_{exp} - q_{cal})^2}{N}} \tag{4}$$

where $q_{exp}$ and $q_{cal}$ are the equilibrium adsorption amounts of metals on the zeolite (mg/g) obtained from experimental work and model calculations, respectively. Lower RMSE values indicate that the results obtained from a model are closer to the actual experimental data.

Based on the RMSE equation and the results in Table 1, it is apparent that the calculated equilibrium adsorption capacity ($Q_{e,c}$) obtained from the pseudo-second-order kinetic model is closer to the experimental adsorption capacity ($Q_{e,e}$). Both the $R^2$ and RMSE suggest that the experimental data are better represented by pseudo-second-order kinetics. Thus, the adsorption behaviors of Pb, Cd, Cu, and Ni on the zeolite are controlled by second-order kinetics, suggesting that the adsorption mechanism involves chemisorption between the adsorbate and the adsorbent. The results also reveal that the adsorption rates, as represented by $k_2$, follow the order of Pb > Cd > Cu > Ni.

Considering that competitive adsorption is a complicated process in a multi-component system, diffusion kinetics models are usually used to evaluate the dynamic behavior. This model can be divided into external and internal diffusion models based on the limiting step of the adsorption process. The internal diffusion model is as follows [34, 36]

$$q_t = k_{id}\sqrt{t} + I \tag{5}$$

Where $q_t$ (mg/g) is the adsorption amount of metal ions on the zeolite at time $t$ (min) and $I$ (mg/g) is a constant. $k_{id}$ (mg/g min$^{1/2}$) is the intra-particle diffusion rate constant.

The external diffusion model may be summarized as [9, 37]:

$$d\ln\frac{C_t}{C_0} = -k_f \frac{A}{V} t + C \tag{6}$$

Where $C_0$ (mg/L) is the initial metal ion concentration, $C_t$ (mg/L) is the concentration at time $t$ (min), $C$ is a constant,
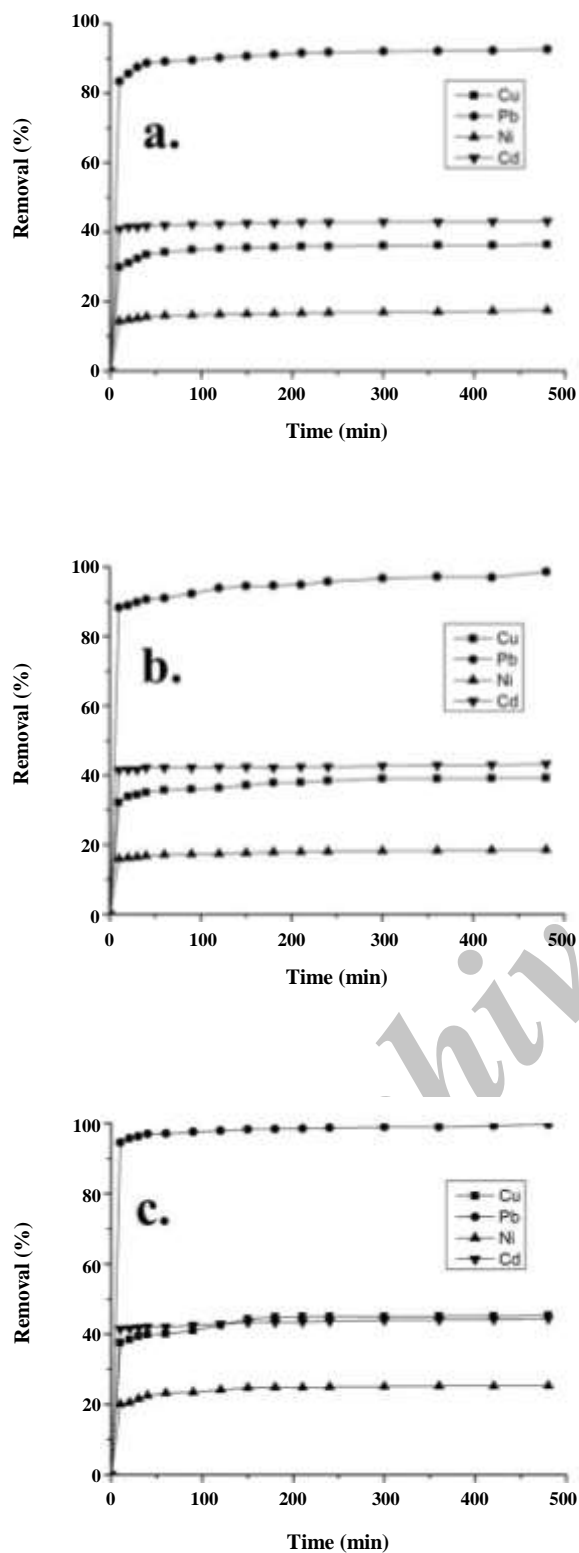
**Fig. 5: Effects of time and temperature on the adsorption of Cu, Ni, Pb, and Cd on the zeolite: (a) 25°C, (b) 35°C, (c) 45°C.**
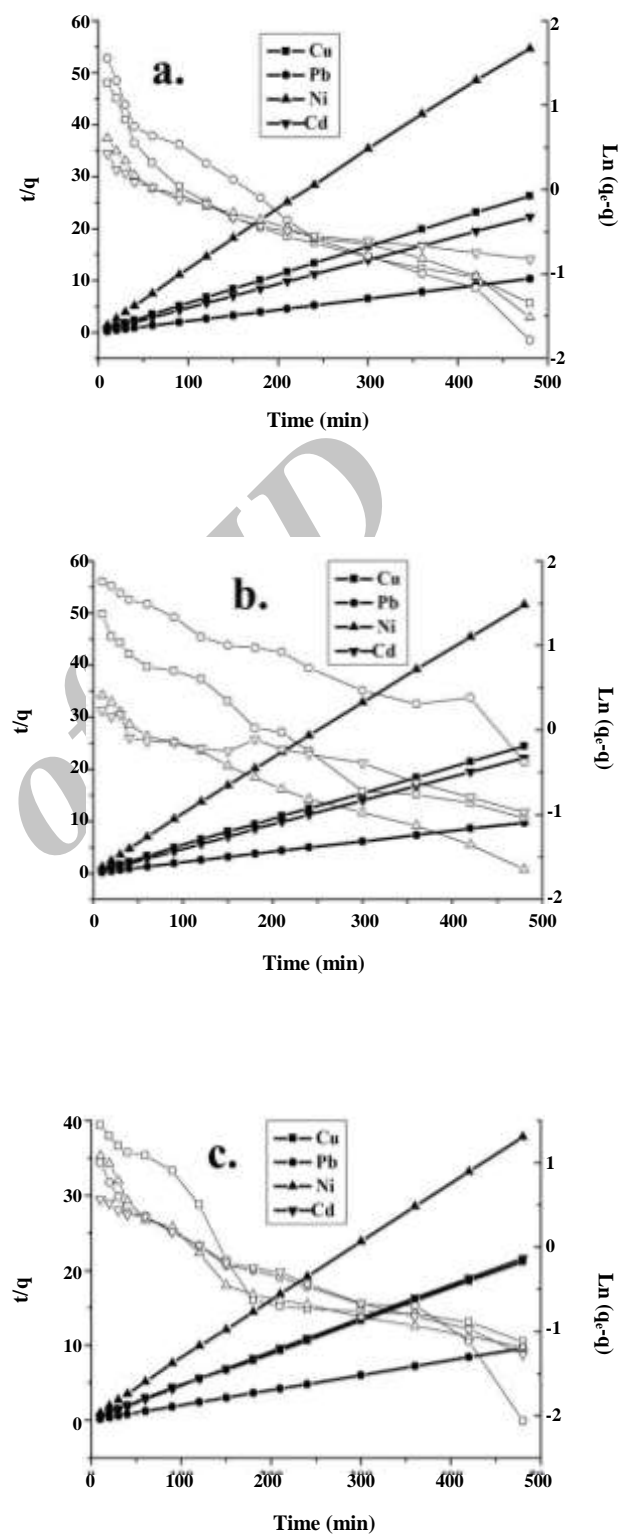
**Fig. 6 Cu, Ni, Pb, and Cd adsorption kinetics on the zeolite, fit using pseudo-first-order plots (empty symbols) and pseudo-second-order plots (filled symbols): (a) 25°C, (b) 35°C, (c) 45°C.**

*Table 1: Kinetic parameters obtained using the pseudo-first-order and pseudo-second-order models.*

| | Temperature(°C) | Pseudo-first-order | | | Pseudo-second-order | | |
|---|---|---|---|---|---|---|---|
| | | $k_1$(1/min) | $q_{cal}$ (mg/g) | $R^2$ | $k_2$(g/mg·min) | $q_{cal}$ (mg/g) | $R^2$ |
| Cu | 25 | 0.0029 | 2.099 | 0.8627 | 0.01753 | 18.315 | 0.9981 |
| | 35 | 0.0041 | 3.1180 | 0.9571 | 0.01934 | 19.841 | 0.9997 |
| | 45 | 0.0048 | 3.2319 | 0.8271 | 0.02101 | 22.935 | 0.0998 |
| Cd | 25 | 0.0031 | 1.1962 | 0.8903 | 0.02421 | 21.598 | 0.9983 |
| | 35 | 0.0044 | 1.1580 | 0.9025 | 0.02449 | 22.563 | 0.9998 |
| | 45 | 0.0058 | 1.6945 | 0.9867 | 0.03508 | 22.221 | 0.9998 |
| Pb | 25 | 0.0049 | 3.1752 | 0.9559 | 0.04705 | 46.511 | 0.997 |
| | 35 | 0.0058 | 5.5339 | 0.9613 | 0.0551 | 49.261 | 0.9998 |
| | 45 | 0.0062 | 2.098 | 0.9337 | 0.06307 | 49.751 | 0.9982 |
| Ni | 25 | 0.0017 | 1.4672 | 0.9497 | 0.01331 | 8.7565 | 0.9995 |
| | 35 | 0.0031 | 1.3125 | 0.9776 | 0.01595 | 9.337 | 0.9997 |
| | 45 | 0.0037 | 1.9823 | 0.8561 | 0.01868 | 12.821 | 0.9998 |

| | $q_{exp}$ (mg/g) | | | RMSE | | |
|---|---|---|---|---|---|---|
| Cu | 25 | 18.5 | | 16.401 | | 0.815 |
| | 35 | 20.2 | | 17.082 | | 0.359 |
| | 45 | 23.4 | | 20.1681 | | 0.465 |
| Cd | 25 | 21.6 | | 20.4038 | | 0.002 |
| | 35 | 21.8 | | 20.642 | | 0.763 |
| | 45 | 22.2 | | 20.5055 | | 0.021 |
| Pb | 25 | 46.5 | | 43.325 | | 0.011 |
| | 35 | 49.5 | | 43.966 | | 0.239 |
| | 45 | 50 | | 47.902 | | 0.249 |
| Ni | 25 | 9.1 | | 7.6328 | | 0.3435 |
| | 35 | 9.5 | | 8.1875 | | 0.163 |
| | 45 | 12.7 | | 10.718 | | 0.121 |

$k_f$ (cm/s) is the external diffusion coefficient and *A/V* is the ratio of the total interfacial area of the particles to the solution volume. This term is calculated as:

$$A/V = 3m/\rho d \tag{7}$$

Where *m* is the adsorbent concentration (g), *d* is the mean particle diameter (μm), and $\rho$ is the apparent density of the adsorbent (g/cm³).

The internal surface diffusion model can be determined from the slope of a straight line fitted to a plot of $\ln(C_t/C_0)$ versus *t*, while the external diffusion model can be obtained from the slope of $q_t$ versus $t^{0.5}$. These kinetics models were applied to the data obtained from the adsorption of Pb, Cu, Cd, and Ni on the zeolite and the results are shown in Figs. 7 and 8 and in Table 2. These data indicate that, prior to the 40-min mark,
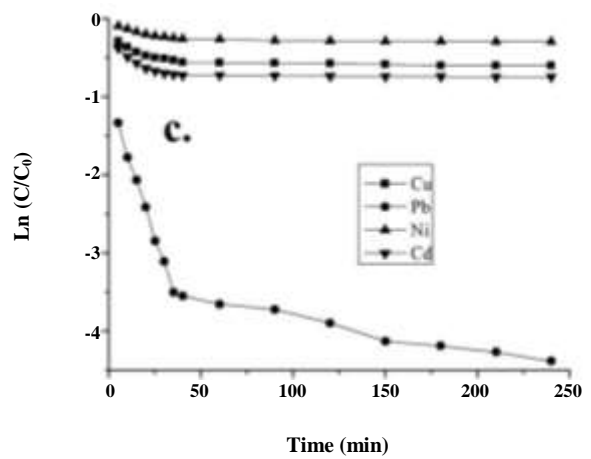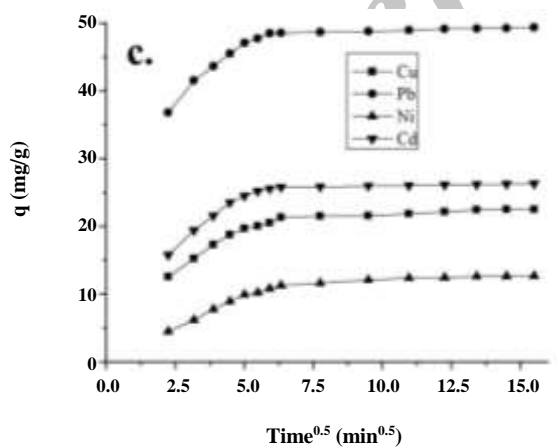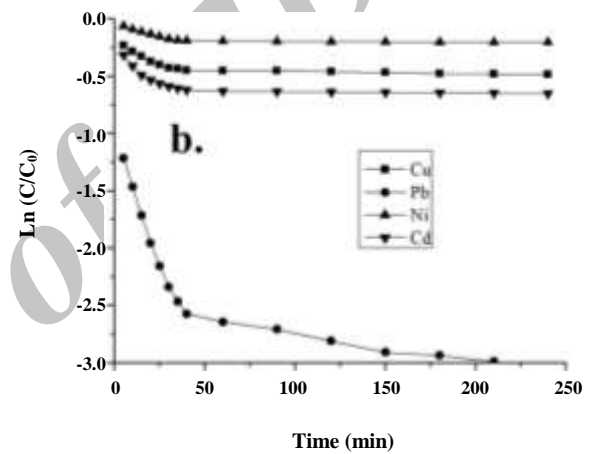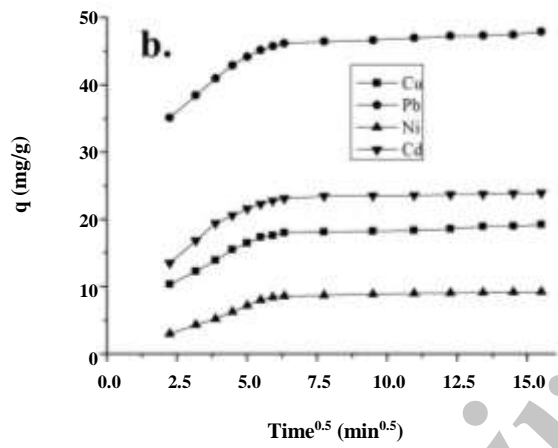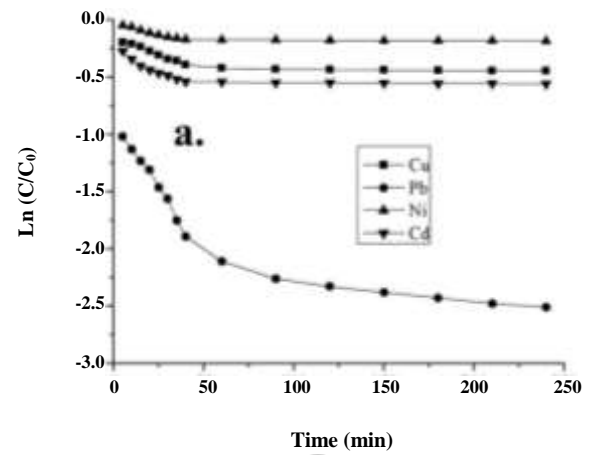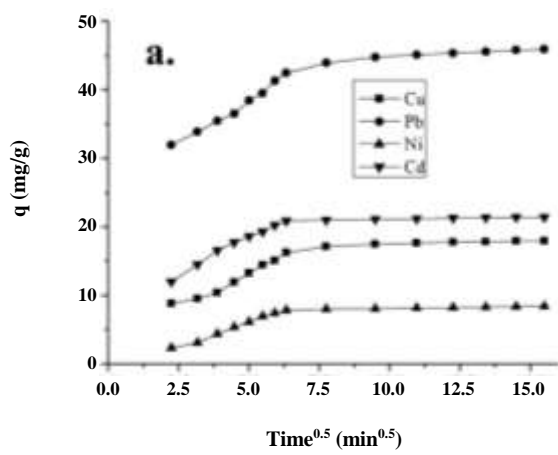
*Fig. 7: Cu, Ni, Pb, and Cd adsorption kinetics on the zeolite, fit using the internal diffusion model: (a) 25°C, (b) 35°C, (c) 45°C.*

*Fig. 8: Cu, Ni, Pb, and Cd diffusion kinetics on the zeolite, fit using the external diffusion model: (a) 25°C, (b) 35°C, (c) 45°C.*

*Table 2: Kinetic parameters obtained using the internal diffusion and external diffusion models.*

| | | Temperature(°C) | External diffusion model | | | Internal diffusion model | | |
|---|---|---|---|---|---|---|---|---|
| | | | $k_f$ (cm/s) | C | $R^2$ | $k_{id}$ (mg/g min$^{1/2}$) | I (mg/g) | $R^2$ |
| 0-40min | Cu | 25 | 0.01579 | -0.1559 | 0.9209 | 1.9114 | 3.7606 | 0.9678 |
| | | 35 | 0.01659 | -0.2254 | 0.9399 | 1.9606 | 6.2569 | 0.9789 |
| | | 45 | 0.01899 | -0.2955 | 0.9165 | 2.0885 | 8.6629 | 0.9629 |
| | Cd | 25 | 0.01927 | -0.2705 | 0.9526 | 2.1389 | 7.7201 | 0.9844 |
| | | 35 | 0.02194 | -0.3315 | 0.899 | 2.3042 | 9.4999 | 0.9429 |
| | | 45 | 0.1271 | -0.3968 | 0.8872 | 2.4473 | 11.51 | 0.9404 |
| | Pb | 25 | 0.06583 | -0.8672 | 0.9275 | 2.577 | 25.706 | 0.9862 |
| | | 35 | 0.1057 | -1.0964 | 0.911 | 2.7396 | 29.871 | 0.9695 |
| | | 45 | 0.1766 | -1.0895 | 0.9261 | 2.8371 | 32.002 | 0.9433 |
| | Ni | 25 | 0.00963 | -0.034 | 0.9196 | 1.4333 | 1.0952 | 0.9914 |
| | | 35 | 0.00990 | -0.053 | 0.937 | 1.4513 | 0.2498 | 0.9903 |
| | | 45 | 0.0120 | -0.0916 | 0.9415 | 1.6763 | 1.062 | 0.9817 |
| 40-240min | Cu | 25 | 0.00042 | -0.4163 | 0.8922 | 0.1049 | 16.425 | 0.8423 |
| | | 35 | 0.00055 | -0.4357 | 0.8699 | 0.1503 | 16.846 | 0.8501 |
| | | 45 | 0.00063 | -0.5476 | 0.7368 | 0.1549 | 20.225 | 0.7491 |
| | Cd | 25 | 0.00023 | -0.5405 | 0.8558 | 0.0591 | 20.532 | 0.8801 |
| | | 35 | 0.00027 | -0.626 | 0.8989 | 0.0621 | 22.923 | 0.7884 |
| | | 45 | 0.00030 | -0.7216 | 0.7895 | 0.0635 | 25.349 | 0.7976 |
| | Pb | 25 | 0.00562 | -2.0466 | 0.8351 | 0.2432 | 42.31 | 0.7479 |
| | | 35 | 0.00723 | -2.474 | 0.762 | 0.1779 | 45.03 | 0.8723 |
| | | 45 | 0.01123 | -3.3985 | 0.7694 | 0.0923 | 47.98 | 0.7674 |
| | Ni | 25 | 0.00016 | -0.1706 | 0.7860 | 0.0592 | 7.5153 | 0.7919 |
| | | 35 | 0.00017 | -0.1895 | 0.8494 | 0.0632 | 8.2753 | 0.7795 |
| | | 45 | 0.00039 | -0.262 | 0.752 | 0.1333 | 10.757 | 0.8107 |

both the internal and external diffusion models can be applied to explain the kinetics of Pb, Cu, Cd, and Ni adsorption on the zeolite, although the internal diffusion model generates better fitting (higher $R^2$). From 40 to 500 min, neither the internal nor external diffusion models generated acceptable results, implying that various diffusion processes are in effect up to 40 min before the metals reach the active adsorption sites of the zeolite. The diffusion process could, therefore, be considered as the rate-determining step of the adsorption kinetics and could be one factor leading to the different adsorption rates of various metals on the zeolite. As the $R^2$ data for the internal diffusion model is better than that for the external diffusion model, the adsorption of metals on the zeolite is evidently best described by the internal diffusion model, in which diffusion through internal channels controls the overall adsorption process. However, in our opinion, external diffusion may also be an important part of the adsorption process and could be the controlling step during the early stages of adsorption from approximately 0 to 2 min.
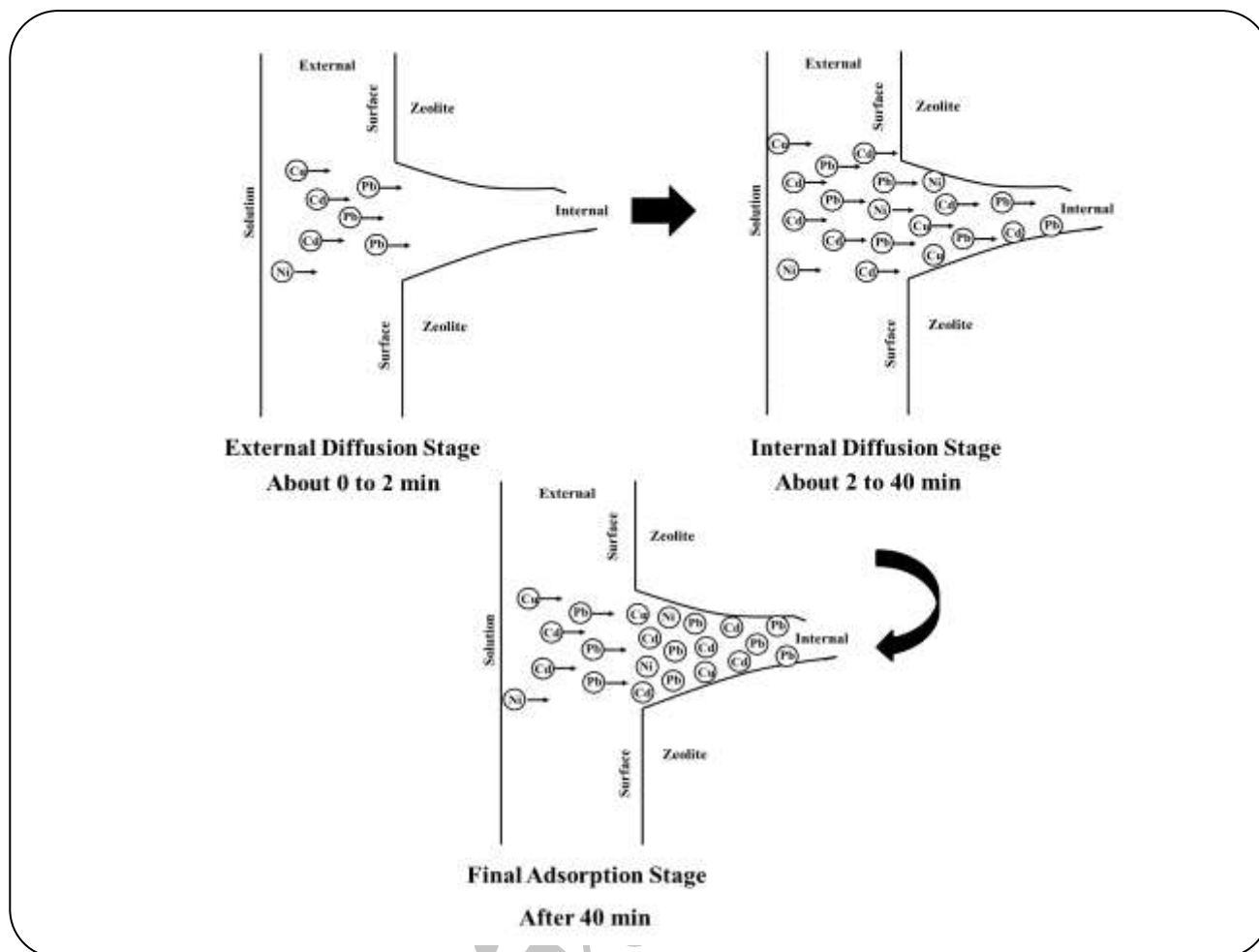
*Fig. 9: Adsorption kinetics model of Cu, Ni, Pb, and Cd on the zeolite.*

Based on the above analysis, it can be seen that the adsorption of metal ions on the zeolite may be divided into two or three stages and that each stage has a different limiting step (see Fig. 9). From the onset of the trial to approximately 0-2 min, the external diffusion model is better suited to the adsorption of Pb, Cu, Cd, and Ni on the zeolite at this stage and that the limiting step is due to external adsorption or boundary layer diffusion. From this point to about 40 min, the correlation coefficient of the internal diffusion model is higher than that of the external diffusion model. This implies that the adsorption process gradually changes from external to internal diffusion. The limiting step of this stage is attributed to internal particle diffusion. Finally, from about 40 min to the final equilibrium stage, neither the external model nor the internal diffusion model gives suitable results, and both $k_f$ and $k_{id}$ decrease to their lowest values. It is possible to speculate that, in this final stage, almost all the adsorption sites on the zeolite have been occupied by metal ions and thus diffusion is no longer the controlling step of the adsorption.

When assessing the adsorption of metals on a zeolite, adsorption isotherms are important. In the present study, we found that the competitive adsorption isotherms of metals on the zeolite are more complicated than those obtained from single metal systems. The common adsorption isotherms functions (including Freundlich and Langmuir isotherm functions) cannot be applied to explain the isotherms of competitive adsorption systems. Thus, more advanced analytic functions and procedures will be applied in our future work, and the associated results will be published in future papers.

**CONCLUSIONS**

It was possible to produce Linde F(K) zeolite from a combination of fly ash and a KOH solution. Cu, Ni, Pb,

70

and Cd ions could be removed from the solution using this zeolite and the adsorption efficiencies decreased in the order of Pb > Cd> Cu > Ni. Higher pH values were found to promote the adsorption process. The metal removal rate is very rapid during the early stages and then gradually decreases, and pseudo-second-order kinetics and internal surface diffusion were determined to best describe the competitive adsorption process. The main adsorption process (from the 1- to 2-min mark to approximately 40 min) is evidently controlled by internal surface diffusion.

## Acknowledgment

## REFERENCES

[1] Huang X., Sillanpää M., Gjessing E. T., Peräniemi S., Vogt R. D., Environmental Impact of Mining Activities on the Surface Water Quality in Tibet : Gyama Valley, *Sci. Total Environ.*, **408**: 4177-4184 (2010).

[2] Ozay O., Ekici S., Baran Y., Aktas N., Sahiner N., Removal of Toxic Metal Ions with Magnetic Hydrogels, *Water Res.*, **43**: 4403-4411 (2009).

[3] Deng P. Y., Liu W., Zeng B. Q., Qiu Y. K., Li L. S., Sorption of Heavy Metals from Aqueous Solution by Dehydrated Powders of Aquatic Plants, *Int. J. Environ. Sci. Technol.*, **10**:559–566 (2013).

[4] Singh K. P., Mohan D., Sinha S., Dalwani R., Impact Assessment of Treated/Untreated Wastewater Toxicants Discharged by Sewage Treatment Plants on Health, Agricultural, and Environmental Quality in the Wastewater Disposal Area, *Chemosphere*, **55**:227-255 (2004).

[5] Hsu P., Leon Y., Antioxidant Nutrients and Lead Toxicity, *Toxicology*, **180**: 33-44 (2002).

[6] Argun M. E., Dursun S., A new Approach to Modification of Natural Adsorbent for Heavy Metal Adsorption, *Bioresour. Technol.*, **99**: 2516-2527 (2008).

[7] Hernández-montoya V., Pérez-cruz M. A., Mendoza-castillo D. I., Moreno-virgen M. R., Competitive Adsorption of Dyes and Heavy Metals on Zeolitic Structures, *J. Environ. Manage.*, **116**: 213-221 (2013).

[8] Prasad M., Xu H., Saxena S., Multi-component Sorption of Pb (II), Cu (II) and Zn (II) onto Low-cost Mineral Adsorbent, *J. Hazard. Mater.*, **154**: 221-229 (2008).

[9] Liu H., Wang C., Liu J., Wang B., Sun H., Competitive Adsorption of Cd(II), Zn(II) and Ni(II) from their binary and ternary acidic systems using tourmaline, *J. Environ. Manage.*, **128**: 727-734 (2013).

[10] Shin K. S., Choi E. M., Taeksung H., Preparation and Characterization of Ion-exchange Membrane Using Sty/HEA/LMA Terpolymer via Post-Sulfonation, *Desalination*, **263**: 151-158 (2010).

[11] Yildiz U., Ferkan Ö., Hazer B., The Removal of Heavy Metal Ions from Aqueous Solutions by Novel pH-sensitive Hydrogels, *J. Hazard. Mater.*, **183**: 521-532 (2010).

[12] Wu N., Li Z., Synthesis and Characterization of Poly (HEA/MALA) Hydrogel and its Application in Removal of Heavy Metal Ions from Water, *Chem. Eng. J.*, **215-216**, 894-902 (2013).

[13] Zhao F., Repo E., Yin D., Sillanpää M. E. T., Adsorption of Cd ( II ) and Pb ( II ) by a Novel EGTA-modified Chitosan Material : Kinetics and Isotherms, *J. Colloid Interface Sci.*, **409**, 174-182 (2013).

[14] Xu H., Liu D., He L., Adsorption of Copper ( II ) from an Wastewater Effluent of Electroplating Industry by Poly (ethyleneimine)-Functionalized Silica, *Iran. J. Chem. Chem. Eng. (IJCCE)*, **34**: 73-81 (2015).

[15] Hossein, F., Marzieh R., Removal of Chromate from Aqueous Solution by a Novel Clinoptilolite-Polyanillin Composite, *Iran. J. Chem. Chem. Eng. (IJCCE)*, **33**, 45-51 (2014).

[16] Solat S., Reza R., Soheila Y., Biosorption of Uranium ( VI ) from Aqueous Solution by Pretreated Aspergillus niger Using Sodium Hydroxide, *Iran. J. Chem. Chem. Eng. (IJCCE)*, **34**, 65-74 (2015).

[17] Cardoso A. M., Paprocki A., Ferret L. S., Azevedo C. M. N., Pires M., Synthesis of Zeolite Na-P1 under Mild Conditions using Brazilian Coal Fly Ash and its Application in Wastewater Treatment, *Fuel*, **139**: 59-67 (2015).

[18] Juan R., Hernández S., Andrés J M., Ruiz C., Synthesis of Granular Zeolitic Materials with High Cation Exchange Capacity from Agglomerated Coal Fly Ash, *Fuel*, 86: 1811-1821 (2007).

[19] Nascimento M., Moreira Soares P S., Paulo de Souza V., Adsorption of Heavy Metal Cations Using Coal Fly Ash Modified by Hydrothermal Method, *Fuel*, **88**: 1714-1719 (2009).

[20] Bhatti H. N., Khadim R., Hanif M. A., Biosorption of Pb(II) and Co(II) on Red Rose Waste Biomass, *Iran. J. Chem. Eng. (IJCCE)*, **30**: 81-87(2011).

[21] Mohammad R., Sasan O., Absorption of Lead Ions by Various Types of Steel Slag, *Iran. J. Chem. Chem. Eng. (IJCCE)*, **27**, 69-75 (2008).

[22] Grela A., Hebda M., Miku J., Thermal Behavior and Physical Characteristics of Synthetic Zeolite from CFB-coal Fly Ash, *Microporous Mesoporpos Mater.*, **220**:155-162 (2016).

[23] Cardoso A. M., Horn M. B., Ferret L. S., Azevedo C. M. N., Integrated Synthesis of Zeolites 4A and Na–P1 using Coal Fly Ash for Application in the Formulation of Detergents and Swine WastewaterTreatment, *J. Hazard. Mater.*, **287**: 69-77 (2015).

[24] Belviso C., Cavalcante F., Gennaro S. D., Lettino A., Palma A., Removal of Mn from Aqueous Solution using Fly Ash and its Hydrothermal Synthetic Zeolite, *J. Environ. Manage.*, **137**: 16-22 (2014).

[25] Chen C., Cheng T., Shi Y., Tian Y., Adsorption of Cu ( II ) from Aqueous Solution on Fly Ash Based Linde F(K) Zeolite, *Iran. J. Chem. Chem. Eng. (IJCCE)*, **33**:29-35 (2014).

[26] Chen C., Cheng T., Wang Z. L., Han C. H., Removal of $Zn^{2+}$ in Aqueous Solution by Linde F(K) Zeolite Prepared from Recycled Fly Ash, *J. Indian Chem. Soc.*, **91**: 1-7 (2014).

[27] Tanaka H., Fujimoto S., Fujii A., Hino R., Kawazoe T., Microwave Assisted Two-Step Process for Rapid Synthesis of Na-A Zeolite from Coal Fly Ash, *Ind. Eng. Chem. Res.*,**47**: 226-230 (2008).

[28] Somerset V. S., Petrik L. F., White R. A., Klink M. J., Key D., Iwuoha E. I., Alkaline Hydrothermal Zeolites Synthesized from High $SiO_2$ and $Al_2O_3$ Co-Disposal Fly Ash Filtrates, *Fuel*, **84**: 2324-2329 (2005).

[29] Eiden-Assmann S., New Heavy Metal-hydro-sodalites Containing $Cd^{2+}$, $Ag^+$ or $Pb^{2+}$: Synthesis by Ion-Exchange and Characterization, *Mat. Res. Bull.*, **37**: 875-889 (2002).

[30] Aljeboree A. M., Alshirifi A. N., Alkaim A. F., Kinetics and Equilibrium Study for the Adsorption of Textile Dyes on Coconut Shell Activated Carbon, *Arab. J. Chem.*, (2014). doi:10.1016/j.arabjc.2014.01.020

[31] Guedidi H., Reinert L., Soneda Y., Bellakhal N., Duclaux L., Adsorption of Ibuprofen from Aqueous Solution on Chemically Surface-modified Activated Carbon Cloths, *Arab. J. Chem.*, **10**:S3584-S3594 (2017).

[32] Zahoor M., Khan F. A., Adsorption of Aflatoxin B1 on Magnetic Carbon Nanocomposites Prepared from Bagasse, *Arab. J. Chem.*, (2014). doi:10.1016/j.arabjc.2014.08.025

[33] Sun D., Zhang X., Wu Y., Liu X., Adsorption of Anionic Dyes from Aqueous Solution on Fly Ash, *J. Hazard. Mater.*, **181**: 335-342 (2010).

[34] Bayo J., Kinetic Studies for Cd(II) Biosorption from Treated Urban Effluents by Native Grapefruit Biomass (Citrus Paradisi L.): The Competitive Effect of Pb(II), Cu(II) and Ni(II), *Chem. Eng. J.*, **191**: 278-287 (2012).

[35] Yu J. X., Wang L. Y., Chi R. A., ZhangY. F., Xu Z. G., Guo J., Competitive Adsorption of $Pb^{2+}$ and $Cd^{2+}$ on Magnetic Modified Sugarcane Bagasse Prepared by Two Simple Steps, *Appl. Surf. Sci.*, **268**:163-170 (2013).

[36] Ho Y. S., Mckay G., Pseudo-second Order Model for Sorption Processes, *Process Biochem.*, **34**: 451–465 (1999).

[37] Al-degs Y. S., El-barghouthi M. I., Issa A. A., Khraisheh M. A., Walker G. M., Sorption of Zn(II), Pb(II), and Co(II) using Natural Sorbents : Equilibrium and Kinetic Studies, *Water Res.*, **40**: 2645-2658 (2006).